AIAA JOURNAL
Vol. 31, No. 1, January 1993

Near-Wall Variable-Prandtl-Number Turbulence Model for Compressible Flows

T. P. Sommer,* R. M. C. So,† and H. S. Zhang*
Arizona State University, Tempe, Arizona 85287

A near-wall variable-Prandtl-number turbulence model is developed for the calculations of high-speed compressible turbulent boundary layers. The model is based on the k-ϵ and the θ^2-$\epsilon_\theta\theta$ equations formulated for near-wall flows. These four equations are used to define the turbulent diffusivities for momentum and heat, thus allowing the assumption of dynamic similarity between momentum and heat transport to be relaxed. The Favre-averaged equations of motions are solved in conjunction with the four transport equations for k, ϵ, θ^2, and ϵ_θ. Calculations are compared with measurements and with other model predictions where the assumption of a constant turbulent Prandtl number is invoked. Incompressible channel/pipe flows and compressible boundary-layer flows with adiabatic as well as constant temperature wall boundary conditions are considered. Cases where the freestream Mach number as high as 10 and where the wall temperature ratio as low as 0.3 are calculated. The analysis shows that the variable Pr_t model yields an asymptotically correct prediction of the temperature variance and the normal heat flux for incompressible flows. In the case of compressible boundary-layer flows, the model calculations are in good agreement with measured mean flow and skin friction for flows with an adiabatic wall and yield substantial improvements in the predictions of mean flow properties compared to the constant Pr_t results for cooled wall cases.

Nomenclature

A^+ = model constant taken to be 45
a_k, b_k = coefficients in the expansion for k^+ in the near-wall region
a_{uv}, b_{uv} = coefficients in the expansion for $\overline{uv}^+$ in the near-wall region
$a_{v\theta}, b_{v\theta}$ = coefficients in the expansion for $\overline{v\theta}^+$ in the near-wall region
a_θ^2, b_θ^2 = coefficients in the expansion for θ^{+2} in the near-wall region
$a_{\epsilon\theta}, b_{\epsilon\theta}$ = coefficients in the expansion for ϵ_θ^+ in the near-wall region
B = constant in law of the wall
$C_{1\lambda}$ = model constant taken to be 0.1
C_{d1} = model constant taken to be 1.8 for boundary layers and 2.0 for internal flows
C_{d2} = model constant taken to be 0
C_{d3} = model constant taken to be 0.72
C_{d4} = model constant taken to be 2.2
C_{d5} = model constant taken to be 0.8
C_f = skin-friction coefficient, $2\tau_w/(\bar\rho U_\infty^2)$
C_h = heat transfer coefficient, $q_w/[(\rho_\infty U_\infty C_p(\Theta_w - \Theta_r)]$
$C_{\epsilon 1}$ = model constant taken to be 1.5
$C_{\epsilon 2}$ = model constant taken to be 1.83
C_μ = model constant taken to be 0.096
C_λ = model constant taken to be 0.11
$f_{w,2}$ = near-wall damping function for ϵ equation
$f_{w,\epsilon\theta}$ = near-wall damping function for ϵ_θ equation
f_μ = near-wall damping function for turbulent momentum diffusivity
f_λ = near-wall damping function for turbulent heat diffusivity
H = instantaneous total enthalpy, $C_pT + ½U_kU_k$
h = half-channel width or pipe radius
k = turbulent kinetic energy
k^+ = normalized k, k/u_τ^2
M = Mach number
M_t = local Mach number, $u_\tau/(\gamma R T_w)^{½}$
P_θ^* = production due to mean temperature, defined as $-\langle u\theta\rangle(\partial\langle\Theta\rangle/\partial x)$
Pr = molecular Prandtl number
Pr_t = turbulent Prandtl number
p = instantaneous pressure
q_w = heat flux at the wall
R = universal gas constant
Re = Reynolds number based on mean bulk velocity, $U_0(2h)/\nu$
Re_t = turbulent Reynolds number, $k^2/(\bar\nu\epsilon)$
Re_τ = Reynolds number based on the wall friction velocity, $u_\tau h/\nu$
R_θ = Reynolds number based on momentum thickness
T = instantaneous temperature
U_0 = mean bulk velocity
U_i = ith component of the instantaneous velocity
U, V = instantaneous velocity components along x and y, respectively
u_i = ith component of the Favre fluctuating velocity
u, v = Favre fluctuating velocity components along x and y, respectively
u^+ = normalized mean U velocity, $\langle U\rangle/u_\tau$
u_c^+ = van Driest coordinate
u_τ = friction velocity, $(\tau_w/\bar\rho_w)^{½}$
$\overline{uv}^+$ = normalized turbulent shear stress, $\langle uv\rangle/u_\tau^2$
$\overline{v\theta}^+$ = normalized turbulent heat flux, $\langle v\theta\rangle/U_\infty\Theta_\infty$
x, y = coordinates along stream and normal directions, respectively
y^+ = normalized y coordinate, $yu_\tau/\bar\nu$
y_w^+ = normalized y coordinate, $yu_\tau/\bar\nu_w$
α = thermal conductivity
α_t = turbulent heat diffusivity
γ = specific heat ratio
δ_r = measured boundary-layer thickness
ϵ = solenoidal dissipation rate of k, $\bar\nu\overline{(\omega_i\omega_i)}$
ϵ_θ = dissipation rate of temperature variance, $\alpha\langle(\partial\theta/\partial x_k)(\partial\theta/\partial x_k)\rangle$
$\tilde\epsilon$ = dissipation rate defined as $\epsilon - 2\bar\nu(\partial\sqrt{k}/\partial y)^2$
$\tilde\epsilon_\theta$ = dissipation rate defined as $\epsilon_\theta - \bar\alpha(\partial\sqrt{\langle\theta^2\rangle}/\partial y)^2$

Received Dec. 18, 1991; revision received May 27, 1992; accepted for publication May 30, 1992.

*Graduate Assistant, Department of Mechanical and Aerospace Engineering

†Professor, Department of Mechanical and Aerospace Engineering.

ϵ^*	= dissipation rate defined as $\epsilon - 2\bar{\nu}k/y^2$
ϵ_θ^*	= dissipation rate defined as $\epsilon_\theta - \bar{\alpha}\theta\langle\theta^2\rangle/y^2$
ϵ^+	= normalized dissipation rate, $\epsilon\bar{\nu}_w/u_\tau^4$
ϵ_θ^+	= normalized dissipation rate, $\epsilon_\theta\bar{\nu}_w/u_\tau^2\Theta_\infty^2$
θ	= Favre fluctuating temperature
$\langle\theta^2\rangle$	= temperature variance
θ^{+2}	= normalized temperature variance, $\langle\theta^2\rangle/\Theta_\infty^2$
$\theta_{\rm rms}^+$	= normalized rms temperature variance, $\sqrt{\langle\theta^2\rangle}/\Theta_\tau$
Θ	= instantaneous temperature
Θ_r	= recovery temperature
Θ_τ	= friction temperature, $q_w/\rho_w\bar{C}_p u_\tau$
Θ^+	= normalized mean temperature, $\langle\Theta\rangle/\Theta_\tau$
κ	= von Kármán constant
μ	= instantaneous fluid viscosity
μ_t	= turbulent viscosity
ν	= instantaneous fluid kinematic viscosity
ν_t	= turbulent kinematic viscosity, μ_t/ρ
ξ	= near-wall correction to ϵ equation
$\xi_{\epsilon\theta}$	= near-wall correction to ϵ_θ equation
ρ	= instantaneous fluid density
ρ'	= Reynolds fluctuating density
σ_k	= model constant taken to be 0.75
σ_ϵ	= model constant taken to be 1.45
σ_{θ^2}	= model constant taken to be 0.75
$\sigma_{\epsilon\theta}$	= model constant taken to be 1.45
τ	= shear stress
ω_i	= fluctuating vorticity
—	= time-averaged quantities
$\langle\ \rangle$	= Favre-averaged quantities

Subscripts

aw	= adiabatic wall
r	= reference condition
w	= wall
∞	= freestream condition

Introduction

IN nonisothermal turbulent flow calculations, turbulent momentum and heat fluxes need modeling if the governing equations are to be closed. If, in addition, the flow is compressible, the modeling of these fluxes is complicated by the presence of a variable mean and fluctuating density in the governing equations. The conventional approach is to neglect the effects of the fluctuating density and to propose models for the momentum fluxes while an additional assumption is made to relate the heat fluxes to the modeled momentum fluxes. Proposals for the incompressible momentum fluxes range from one-equation to second-order closure models.[1] Most closure schemes for compressible flows invoke Morkovin's hypothesis[2] of dynamic field similarity between compressible and incompressible flows. Therefore, this assumption allows the direct extension of incompressible models to account for compressibility effects. In addition, the assumption of dynamic similarity between turbulent heat and momentum transport is invoked, and this permits the specification of a constant Pr_t in the closure schemes.[3-8] Under these assumptions, compressibility effects are accounted for by the mean density alone. As a result, the ability of conventional models to reliably predict compressible turbulent boundary-layer flows for Mach numbers $M_\infty \geq 5$ has been called into question.[9]

Attempts to relax some of these assumptions have been made recently. For example, Zhang et al.[10] propose a compressible near-wall k-ϵ model for flat plate boundary-layer flows. Their analysis reveals that, if the near-wall model is internally consistent and asymptotically correct, Morkovin's hypothesis is essentially valid for an adiabatic wall boundary condition with M_∞ as large as 10. Consequently, the predictions in this Mach number range are in good agreement with measurements. On the other hand, the model predictions of cooled wall boundary layers at high Mach numbers are not as good. The reason may not be the breakdown of Morkovin's hypothesis, but rather the consequence of the assumption of a constant Pr_t. The present study makes a first attempt to assess this postulate and proposes to relax the assumption of a constant Pr_t in the modeling of compressible turbulent boundary layers. A near-wall variable Pr_t model is suggested as an alternative, where a compressible k-ϵ model is used to resolve the turbulent shear stress and a recently developed incompressible θ^2-ϵ_θ model is extended to calculate the compressible turbulent heat flux.

A number of near-wall two-equation k-ϵ models[11-16] are available. However, none is as widely tested for asymptotic consistency as the model of So et al.,[15] who have validated their model against such benchmark data as direct numerical simulations of channel flows,[17,18] of flat plate boundary-layer flows,[19] and of Couette flows[20] as well as experimental measurements.[21,22] Their results are in excellent agreement with data and have been recently reported.[15,23-25] In view of this, Zhang et al.[10] adopt the near-wall model of So et al.[15] and extend it directly to compressible flows. Therefore, this suggests that the compressible near-wall k-ϵ model of Zhang et al.[10] should be adopted for the modeling of the momentum fluxes in the present study.

If constant Pr_t is not assumed, a near-wall heat flux model has to be proposed. Near-wall modeling of heat fluxes is not as well developed; nevertheless, a second-order closure[26] and a two-equation θ^2-ϵ_θ model[27] have been put forward for nonisothermal incompressible flows. In these models the assumption of a vanishing wall fluctuating temperature is invoked. This assumption is only valid for adiabatic wall and is not appropriate for other wall boundary conditions. Consequently, an alternative model has been proposed to remedy this assumption.[28] However, none has been formulated for compressible flows at present. The work of Zhang et al.[10] points to the importance of having an internally consistent and asymptotically correct near-wall model for compressible flows. Therefore, if an incompressible near-wall θ^2-ϵ_θ model is to be extended to compressible boundary layers, its asymptotic behavior near a wall has to be analyzed first. This analysis has been carried out for the θ^2-ϵ_θ model[29] and the results show that the model of Ref. 27 fails to correctly reproduce the asymptotic behavior of the temperature variance and its dissipation rate. Sommer et al.[29] propose modifications along the line of the analysis of the ϵ equation given by So et al.[15] and derive a correction function for the ϵ_θ equation by extending the coincidence condition of Shima[30] to the analysis of the ϵ_θ equation. Thus derived, the new near-wall θ^2-ϵ_θ model is found to correlate well with direct simulation results,[31,32] and experimental measurements.[33,34] In particular, the asymptotic near-wall behavior of the direct simulation data is reproduced correctly for both constant temperature and constant heat flux wall boundary conditions. The present objective is to extend the near-wall θ^2-ϵ_θ model[29] to compressible flows. This is accomplished by adopting the approach used in Ref. 10 and applying it to treat the incompressible θ^2 and ϵ_θ equations so that they can be extended to compressible flows.

The variable Pr_t model is used to calculate incompressible and compressible turbulent flows with adiabatic, constant heat flux and constant temperature wall boundary conditions. For incompressible flows the calculations are compared with direct numerical simulation (DNS) data[32] and experimental measurements,[33,34] where accurate near-wall profiles of $\langle\Theta\rangle$ and $\langle v\theta\rangle$ are available. Compressible flow calculations are validated against well-documented experimental measurements[35,36] and also against constant Pr_t model calculations of the k-ϵ type[10] and k-ω type.[37] Therefore, the validity and extent of the constant Pr_t assumption can be critically assessed.

Compressible Boundary-Layer Equations

The mean equations of motions for compressible turbulent boundary layers can be derived from the instantaneous

Navier-Stokes equations by applying Favre averaging and then invoking the Prandtl boundary-layer approximations to simplify the resultant averaged equations. Favre decomposition is invoked for all variables except p and ρ where conventional Reynolds decomposition is assumed. When these decompositions are substituted into the Navier-Stokes equations and time averaging is applied, a set of turbulent mean flow equations is obtained. The boundary-layer approximations and the assumption of negligible fluctuations in fluid properties, such as μ and C_p, are used to further simplify these equations. Since the pressure field is constant for flat-plate boundary layers, the resultant compressible turbulent boundary-layer equations can be written as:

$$\frac{\partial}{\partial x}(\bar{\rho}\langle U\rangle)+\frac{\partial}{\partial y}(\bar{\rho}\langle V\rangle)=0 \tag{1}$$

$$\bar{\rho}\langle U\rangle\frac{\partial\langle U\rangle}{\partial x}+\bar{\rho}\langle V\rangle\frac{\partial\langle U\rangle}{\partial y}=\frac{\partial}{\partial y}\left[(\bar{\mu}+\bar{\mu}_t)\frac{\partial\langle U\rangle}{\partial y}\right] \tag{2}$$

$$\begin{aligned}\bar{\rho}\langle U\rangle\frac{\partial\langle H\rangle}{\partial x}+\bar{\rho}\langle V\rangle\frac{\partial\langle H\rangle}{\partial y}&=\frac{\partial}{\partial y}\left[\left(\frac{\bar{\mu}}{Pr}+\frac{\bar{\mu}_t}{Pr_t}\right)\frac{\partial\langle H\rangle}{\partial y}\right.\\ &\left.+\left\{\bar{\mu}\left(1-\frac{1}{Pr}\right)+\bar{\mu}_t\left(1-\frac{1}{Pr_t}\right)\right\}\langle U\rangle\frac{\partial\langle U\rangle}{\partial y}\right]\\ &+\frac{\partial}{\partial y}\left[\left\{\bar{\mu}\left(1-\frac{1}{Pr}\right)+\bar{\mu}_t\left(\frac{1}{\sigma_k}-\frac{1}{Pr_t}\right)\right\}\frac{\partial k}{\partial y}\right]\end{aligned} \tag{3}$$

The mean equation of state is assumed to be given by $\bar{p}=\bar{\rho}R\langle\Theta\rangle$. Sutherland's law is used to evaluate the mean fluid viscosity when the working fluid is air, whereas a power law is used when the working fluid is helium. Therefore, once $\bar{\mu}_t$ and Pr_t are known, Eqs. (1-3) can be solved to give the velocity and temperature fields inside the boundary layers.

In writing down these equations, gradient transport has been assumed for the turbulent momentum and heat fluxes. Therefore, if $\bar{\mu}_t$ is taken to be given by $\bar{\rho}(\bar{\nu}_t)$, the turbulent fluxes can be written as

$$-\bar{\rho}\langle uv\rangle=\bar{\rho}\bar{\nu}_t\frac{\partial\langle U\rangle}{\partial y} \tag{4a}$$

$$-\bar{\rho}\langle v\theta\rangle=\bar{\rho}\frac{\bar{\nu}_t}{Pr_t}\frac{\partial\langle\Theta\rangle}{\partial y} \tag{4b}$$

Even though Eqs. (1-4) are written in terms of Pr_t, they do not imply constant Pr_t. The equations are simply written in this form for convenience and to comply with conventional format. Here, $Pr_t=\bar{\nu}_t/\bar{\alpha}_t$, and the turbulent diffusivities are defined as:

$$\bar{\nu}_t=C_\mu f_\mu k^2/\epsilon \tag{5a}$$

$$\bar{\alpha}_t=C_\lambda f_\lambda k\,[k\langle\theta^2\rangle/\epsilon\epsilon_\theta]^{1/2} \tag{5b}$$

where the damping functions are defined later in the discussion of closure models for the momentum and heat fluxes. Consequently, Pr_t varies according to the distributions of $\bar{\nu}_t$ and $\bar{\alpha}_t$, which can be determined from asymptotically consistent near-wall turbulence models to be proposed for these diffusivities.

Consistent with conventional wisdom, the temperature equation is converted into the total enthalpy equation. It should be pointed out that a rigorous derivation of Eq. (3) leads to an additional $\partial k/\partial y$ term on the right-hand side of Eq. (3). In the past, researchers[3,6,8] have argued that this term is small compared to the mean velocity term on the right-hand side and can therefore be neglected. Recently, calculations[10] have shown that this term is unimportant in compressible boundary layers with M_∞ as large as 10 and Θ_w/Θ_{aw} as small as 0.3. The term also vanishes identically when $Pr=1$ and $\sigma_k=Pr_t$. Therefore, the $\partial k/\partial y$ term in Eq. (3) is neglected in the present formulation so that a true evaluation of the variable Pr_t effect can be made compared to other model calculations.

The boundary conditions for $\langle U\rangle$ and $\langle V\rangle$ are no slip at the wall and $\langle U\rangle$ approaches U_∞ in the freestream. As for $\langle H\rangle$, its freestream value is given by $H_\infty=C_p\Theta_\infty+U_\infty^2/2$, and its wall value is taken to be either that of an adiabatic wall or a specified constant H_w.

Near-Wall k-ϵ Turbulence Model for $\bar{\nu}_t$

In adopting and extending the near-wall k-ϵ model of So et al.[15] to compressible flows, Zhang et al.[10] found that dilatational effects in the near-wall region can be accounted for by the varying mean density alone. Furthermore, they found that the additional dilatational terms in the modeled equations have very little effect on compressible boundary-layer calculations in the Mach number range $0\le M_\infty\le 10$ and wall temperature ratio range $0.2\le\Theta_w/\Theta_{aw}\le 1.0$. Therefore, as a first attempt, it is prudent to calculate turbulent heat fluxes using a near-wall model where the additional dilatational terms are neglected. In view of this, the near-wall k-ϵ model of Zhang et al.[10] without the dilatational terms are adopted for the present study. The modeled k-ϵ equations for boundary-layer flows can be written as

$$\bar{\rho}\langle U\rangle\frac{\partial k}{\partial x}+\bar{\rho}\langle V\rangle\frac{\partial k}{\partial y}=\frac{\partial}{\partial y}\left[\left(\bar{\mu}+\frac{\bar{\mu}_t}{\sigma_k}\right)\frac{\partial k}{\partial y}\right]+\bar{\mu}_t\left(\frac{\partial\langle U\rangle}{\partial y}\right)^2-\bar{\rho}\epsilon \tag{6}$$

$$\begin{aligned}\bar{\rho}\langle U\rangle\frac{\partial\epsilon}{\partial x}+\bar{\rho}\langle V\rangle\frac{\partial\epsilon}{\partial y}&=\frac{\partial}{\partial y}\left[\left(\bar{\mu}+\frac{\bar{\mu}_t}{\sigma_\epsilon}\right)\frac{\partial\epsilon}{\partial y}\right]\\ &+C_{\epsilon1}\frac{\epsilon}{k}\bar{\mu}_t\left(\frac{\partial\langle U\rangle}{\partial y}\right)^2-C_{\epsilon2}\bar{\rho}\left(\frac{\epsilon\tilde{\epsilon}}{k}\right)+\xi\end{aligned} \tag{7}$$

where ξ is defined as

$$\xi=f_{w,2}\bar{\rho}\left[-2\frac{\epsilon\tilde{\epsilon}}{k}+1.5\frac{\epsilon^{*2}}{k}\right] \tag{8}$$

Here, $f_{w,2}=e^{-(R_t/64)^2}$ is a damping function that asymptotes to one at the wall and zero far away from the wall. The boundary conditions for k and ϵ are zero values in the freestream. At the wall, $k=0$ is assumed, and ϵ is taken to be given by $2\bar{\nu}_w(\partial\sqrt{k}/\partial y)_w^2$.

Once k and ϵ are known, they can be used to evaluate $\bar{\nu}_t$ according to Eq. (5a) and hence $\bar{\mu}_t=\bar{\rho}\bar{\nu}_t$. The damping function f_μ associated with $\bar{\nu}_t$ is given as[15]

$$f_\mu=(1+3.45/\sqrt{R_t})\tanh(y^+/115) \tag{9}$$

This damping function behaves correctly as a wall is approached, i.e., f_μ goes like y^{-1} as y approaches zero. In other words, the modeled turbulent shear stress again behaves like y^3 near a wall similar to its exact behavior.

Near-Wall θ^2-ϵ_θ Turbulence Model for $\bar{\alpha}_t$

A detailed derivation of the incompressible near-wall θ^2-ϵ_θ model has already been given.[29] Consequently, there is no need to repeat the derivation here. However, some major differences between the the k-ϵ equations and the θ^2-ϵ_θ equations should be pointed out. The first is the modeling of the generation and destruction terms in the ϵ_θ equation. Since thermal and velocity time scales are of equal importance in turbulent heat transfer, both time scales are used in the modeling of the generation and destruction terms. A second difference is in the wall boundary conditions. Constant heat flux and constant temperature wall boundary condition can be specified for nonisothermal flows. Therefore, these differences have to be taken into account in the derivation of a near-wall correction for the ϵ_θ equation. Sommer et al.[29] extend the coincidence condition of Shima[30] to treat the ϵ_θ equation and derive a near-wall correction function for the ϵ_θ equation in a manner similar to that used by So et al.[15] in their derivation of ξ. Thus formulated, the $\overline{\theta^2}$ and ϵ_θ equations behave correctly as a wall is approached, at least to the lowest order of y.

The incompressible near-wall θ^2-ϵ_θ model for α_t can be extended to compressible flows in the following manner. Again, fluctuating temperature and density are assumed to go to zero simultaneously at the wall and fluctuating fluid properties are neglected. Therefore, all fluid properties, such as μ, C_p, etc., can be replaced by their time-averaged values and the following near-wall expansions can be assumed for the fluctuating quantities:

$$u = a_1 y + a_2 y^2 + \tag{10a}$$

$$v = b_1 y + b_2 y^2 + \tag{10b}$$

$$\theta = c_1 y + c_2 y^2 + \tag{10c}$$

$$\rho' = d_1 y + d_2 y^2 + \tag{10d}$$

where a, b, c, and d are random functions of x, z, and t. As pointed out by Bradshaw,[38] θ and ρ' cannot go to zero simultaneously at the wall; otherwise it would lead to a zero wall p', which is not physically possible. In general, θ is taken to vanish at the wall, but ρ' is not. Here, ρ' is also assumed to be zero at the wall; however, its value away from the wall is finite. Therefore, this assumption represents an improvement of Morkovin's hypothesis[2] which neglects the influence of fluctuating density altogether in the whole flow. Under this assumption and with the help of the continuity equation for ρ' and Eq. (10), it can be easily shown that b_1 is identically zero irrespective of the wall thermal boundary conditions. This means that the near-wall asymptotic analysis of So et al.[15] can be used to examine the exact and modeled compressible θ^2 and ϵ_θ equations in the near-wall region. The result is similar to that given by Sommer et al.[29] for the incompressible case. Therefore, the incompressible form of the near-wall θ^2 and ϵ_θ equations can be directly extended to compressible flows just as in the case of the k and ϵ equations.

In view of this, the compressible θ^2 and ϵ_θ equations can be written as[29]

$$\bar\rho\langle U\rangle \frac{\partial\langle\theta^2\rangle}{\partial x} + \bar\rho\langle V\rangle \frac{\partial\langle\theta^2\rangle}{\partial y} = \frac{\partial}{\partial y}\left(\bar\rho\bar\alpha \frac{\partial\langle\theta^2\rangle}{\partial y}\right) + \frac{\partial}{\partial y}\left(\frac{\bar\rho\bar\alpha_t}{\sigma_{\theta 2}} \frac{\partial\langle\theta^2\rangle}{\partial y}\right)$$
$$+ 2\bar\rho\bar\alpha_t\left(\frac{\partial\langle\Theta\rangle}{\partial x}\right)^2 + 2pd_t\left(\frac{\partial\langle\theta\rangle}{\partial y}\right)^2 - 2\bar\rho\epsilon_\theta \tag{11}$$

$$\bar\rho\langle U\rangle \frac{\partial\epsilon_\theta}{\partial x} + \bar\rho\langle V\rangle \frac{\partial\epsilon_\theta}{\partial y} = \frac{\partial}{\partial y}\left(\bar\rho\bar\alpha \frac{\partial\epsilon_\theta}{\partial y}\right) + \frac{\partial}{\partial y}\left(\frac{\bar\rho\bar\alpha_t}{\sigma_{\epsilon\theta}} \frac{\partial\epsilon_\theta}{\partial y}\right)$$
$$+ C_{d1}\frac{\epsilon_\theta}{\langle\theta^2\rangle}\bar\rho\bar\alpha_t\left(\frac{\partial\langle\Theta\rangle}{\partial x}\right)^2 + C_{d1}\frac{\epsilon_\theta}{\langle\theta^2\rangle}\bar\rho\bar\alpha_t\left(\frac{\partial\langle\Theta\rangle}{\partial y}\right)^2$$
$$+ C_{d2}\frac{\epsilon}{k}\bar\rho\bar\alpha_t\left(\frac{\partial\langle\Theta\rangle}{\partial y}\right)^2 + C_{d3}\frac{\epsilon_\theta}{\langle k\rangle}\mu_t\left(\frac{\partial\langle U\rangle}{\partial y}\right)^2$$
$$- C_{d4}\frac{\tilde\epsilon_\theta}{\langle\theta^2\rangle}\bar\rho\epsilon_\theta - C_{d5}\frac{\tilde\epsilon}{k}\bar\rho\epsilon_\theta + \xi_{\epsilon\theta} \tag{12}$$

where the near-wall correction function $\xi_{\epsilon\theta}$ is given by

$$\xi_{\epsilon\theta} = f_{w,\epsilon\theta}\bar\rho\left[(C_{d4}-4)\frac{\tilde\epsilon_\theta}{\langle\theta^2\rangle}\epsilon_\theta + C_{d5}\frac{\tilde\epsilon}{k}\epsilon_\theta - \frac{\epsilon_\theta^{*2}}{\langle\theta^2\rangle}\right.$$
$$\left. + (2 - C_{d1} - C_{d2}Pr)\frac{\epsilon_\theta}{\langle\theta^2\rangle}P_\theta^*\right] \tag{13}$$

The damping function is defined as $f_{w,\epsilon\theta} = \exp[-(Re_t/80)^2]$, and $\bar\alpha_t$ is given by Eq. (5b). To recover the exact behavior of $\langle v\theta\rangle$ near a wall, $\bar\alpha_t$ has to behave like y^3 near a wall; therefore, this requires the damping function f_λ in Eq. (5b) to go like y^{-1} as y approaches zero. The damping function f_λ thus derived is given as[29]

$$f_\lambda = \left[f_{w,\epsilon\theta}\frac{C_{1\lambda}}{\sqrt[4]{Re_t}}\right] + [1 - \exp(-y^+/A^+)]^2 \tag{14}$$

Boundary conditions for $\langle\theta^2\rangle$ and ϵ_θ are zero values in the freestream and vanishing $\langle\theta^2\rangle$ at the wall. As for ϵ_θ, its value at the wall is given by $\bar\alpha_w[(\partial\sqrt{\langle\theta^2\rangle}/\partial y)^2]_w$.

Results and Discussion

The governing equations [(1–7), (11), and (12)] are solved for the present variable Pr_t model. Exact boundary conditions at the wall for the turbulence quantities are used because, with near-wall corrections proposed in Eqs. (8) and (13), the equations can be integrated directly to the wall. To evaluate the merit of a variable Pr_t, validations are carried out with both incompressible and compressible flow data and also with two other model calculations, where $Pr_t = 0.9$ is assumed. The first is the k-ϵ model of Ref. 10 that solves Eqs. (1–7), whereas the second is the k-ω model where the modeled equations given in Ref. 37 are solved. Whenever there are significant differences between the k-ϵ and k-ω calculations, both sets of results are plotted for comparison; if not, only the k-ϵ results are compared with data.

According to Refs. 15 and 29, near a wall, the quantities k, $\langle uv\rangle$, ϵ, $\langle\theta^2\rangle$, $\langle v\theta\rangle$, and ϵ_θ can be expanded in terms of y. After proper normalization using wall variables, the expansions for both incompressible and compressible flows can be written as[15,29]

$$k^+ = a_k(y_w^+)^2 + b_k(y_w^+)^3 + \cdots \tag{15}$$

$$\overline{uv}^+ = a_{uv}(y_w^+)^3 + b_{uv}(y_w^+)^4 + \cdots \tag{16}$$

$$\epsilon^+ = 2a_k + 4b_k y_w^+ + \cdots \tag{17}$$

$$\theta^{+2} = a_\theta(y_w^+)^2 + b_\theta(y_w^+)^3 + \cdots \tag{18}$$

$$\overline{v\theta}^+ = a_{v\theta}(y_w^+)^3 + b_{v\theta}(y_w^+)^4 + \cdots \tag{19}$$

$$\epsilon_\theta^+ = a_{\epsilon\theta} + b_{\epsilon\theta}y_w^+ + \ldots \tag{20}$$

where the Favre average reduces to the Reynolds average for incompressible flows. The accuracy with which the near-wall asymptotics, such as a_k, a_{uv}, a_θ, $a_{v\theta}$, and $a_{\epsilon\theta}$, can be predicted is a measure of the correctness of the variable Pr_t model. Furthermore, $k^+/\epsilon^+(y_w^+)^2$ and $\theta^{+2}/\epsilon_\theta^+(y_w^+)^2$ at the wall are exactly equal to 0.5 and Pr, respectively, and the results are independent of Re and the turbulence model. It has been shown that the k-ϵ model gives reasonable values for a_k and a_{uv} compared to DNS data.[15] Since the same validation has also been carried out for the θ^2 and ϵ_θ equations for incompressible flows,[29] the present objective is to show that the values calculated for a_θ, $a_{v\theta}$, and $a_{\epsilon\theta}$ are reasonable and that $\theta^{+2}/\epsilon_\theta^+(y_w^+)^2$ is evaluated to be equal to Pr for compressible flows. In the process, Eqs. (11) and (12) can be demonstrated to be asymptotically correct for incompressible as well as compressible flows.

Incompressible Flow Results

Since a generally thorough evaluation of the variable Pr_t model with incompressible DNS data and other near-wall θ^2-ϵ_θ models has been carried out in Ref. 29, the present investigation concentrates only on comparing the relative performance of the variable and constant Pr_t models in their predictions of DNS data.[32] In addition, the models' ability to correctly calculate incompressible pipe flows at high Reynolds number[33,34] is also analyzed. In the DNS flow case, $Re_\tau = 1.5 \times 10^2$, $Re =$

4.56×10^3, and $Pr = 0.71$, while the experimental cases given in Refs. 33 and 34 have $Re = 49.5$ and 4×10^4, respectively. All three cases have a constant wall heat flux wall boundary condition. These flow cases are calculated using the computer code of Ref. 26. The code applies a Newton linearization scheme to solve the set of ordinary differential equations obtained for fully developed flows and has been shown to give grid-independent solutions when the grid points are distributed in the following manner: 5 points in the region $0 \le y^+ \le 5$; 15 points in the region $5 \le y^+ \le 65$; and about 50 points in the region $65 \le y^+ \le Re$. An initial guess of the distributions of the dependent variables is specified together with an appropriate Re_τ. Iteration is carried out until the maximum relative change of all of the variables at every grid point satisfies an accuracy criterion of 10^{-5} or less. In these test cases the mean temperature and the normal heat flux are measured independently. Therefore, they represent a true evaluation of the validity and extent of the variable Pr_t model.

From the DNS data,[32] the following near-wall asymptotics can be determined: $a_\theta = 0.068$, $a_{\epsilon\theta} = 0.097$, and $\theta^{+2}/\epsilon_\theta^+(y_w^+)^2 = 0.71$. These values are consistent with those reported by Antonia and Kim[39] for the case with constant wall temperature boundary condition. The corresponding values deduced from the variable Pr_t model are 0.053, 0.074, and 0.71, respectively. Other near-wall asymptotics thus calculated are $a_{v\theta} = 8.9 \times 10^{-4}$, $a_k = 0.086$, $a_{uv} = 8.4 \times 10^{-4}$, and $k^+/\epsilon^+(y_w^+)^2 = 0.5$. The constant Pr_t model predictions of these properties are 6.7×10^{-4}, 0.086, 8.4×10^{-4}, and 0.5, respectively. With the exception of $a_{v\theta}$, the calculations of both the constant and variable Pr_t models are in excellent agreement with each other. This is not surprising because the same basic k-ϵ model is used in both the constant and variable Pr_t models. On the other hand, the prediction of $a_{v\theta}$ by the variable Pr_t model appears to be in good agreement with DNS data as evidence by the calculated normal heat flux shown in Fig. 1b. Furthermore, the prediction of $\theta^{+2}/\epsilon_\theta^+(y_w^+)^2$ is exactly correct, thus verifying that the variable Pr_t model is asymptotically consistent.

Comparisons of the mean temperature and normal heat flux are shown in Figs. 1-3. The variable Pr_t model yields a slightly better prediction of the mean temperature for the DNS flow case. However, both models fail to correctly predict the intercept of the log law; this failure can be attributed to a low Reynolds number effect (Fig. 1a). This point is substantiated by the high Reynolds number comparisons given in Fig. 2. Here, the calculations are carried out for fully developed pipe flow with heat transfer at a $Re = 49.5 \times 10^4$. The variable Pr_t model gives a slightly better prediction of the data than the constant Pr_t model. Further calculations over a range of Re varying from 24.9×10^4 to 71.2×10^4 yield essentially the same improvement compared to measurements.[33] According to Ref. 33, the thermal von Kármán constant varies fron 0.47 to 0.55 over this range of Re. This dependence on Re of the thermal von Kármán constant is also correctly predicted. Additional evidence in support of this claim can be gleaned from a comparison of the calculated near-wall heat flux with some recent measurements.[34] This result is shown in Fig. 3 and, again, the variable Pr_t model gives a better prediction of the normal heat flux; in particular, the maximum reached in the near-wall region. In general, the calculations of the variable Pr_t model are in good agreement with the normal heat flux data (Figs. 1b and 3).

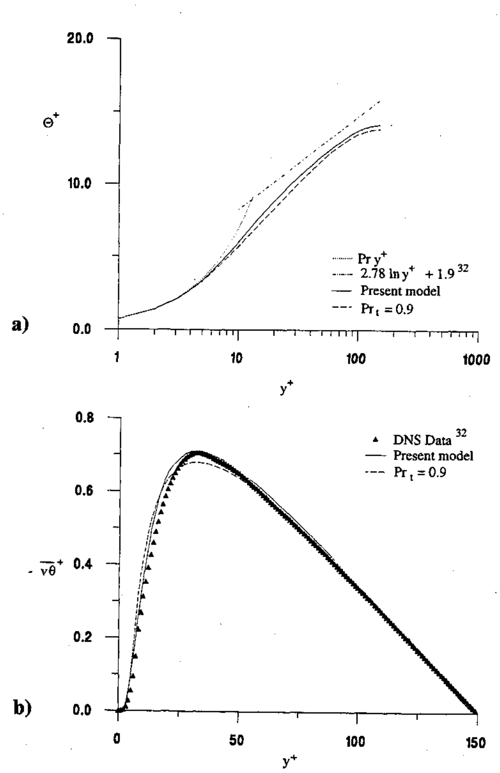

Fig. 1 Comparison of the calculated mean velocity and normal heat flux with DNS data: a) Θ^+; b) $\langle v\theta \rangle$.

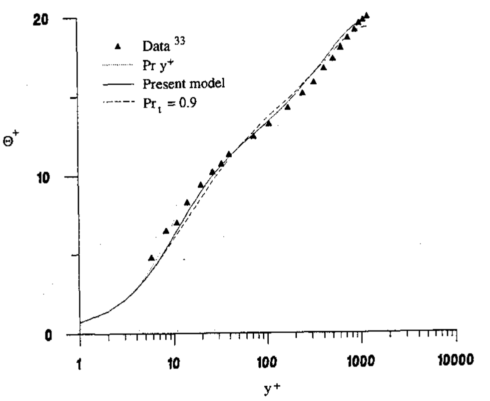

Fig. 2 Comparison of the calculated mean velocity with measurements.

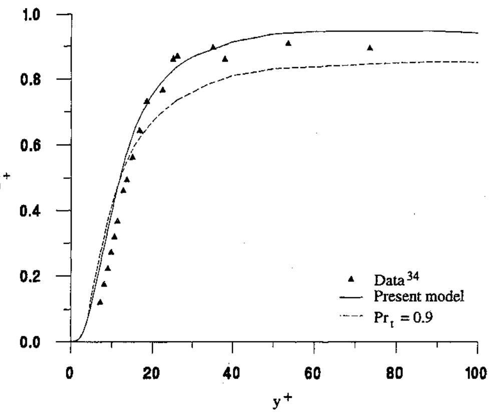

Fig. 3 Comparison of the calculated normal heat flux with measurements.

Compressible Flow Results

For compressible flows, one case from Ref. 35 is chosen and three cases are selected from Ref. 36. The case from Ref. 35 is specified by $\Theta_w/\Theta_{aw} = 0.30$, $M_\infty = 8.19$, and $R_\theta = 4.6 \times 10^3$ and the mean temperature is measured independent of the mean velocity. Air is the working fluid, therefore, Sutherland's law is used to calculate the mean viscosity and $Pr = 0.74$. Two cases with an adiabatic wall boundary condition are selected from Ref. 36 and they are labeled as cases 53011302 and

73050504. The freestream Mach numbers for these two cases are 4.544 and 10.31, respectively, and the corresponding R_θ are 5.532×10^3 and 15.074×10^4. Since the fluid medium of case 53011302 is air, Sutherland's law is used to evaluate the mean viscosity and $Pr=0.74$ is specified. On the other hand, helium is used in the experiments of case 73050504; therefore, $Pr=0.70$ and a power law[36] is used to calculate the mean viscosity. In these experiments, the mean temperature profiles are inferred from the measured mean velocity profiles and the assumption of constant $\langle H\rangle$. The third case is specified by $\Theta_w/\Theta_{aw}=0.92$, $M_\infty=5.29$, and $R_\theta=3.939\times10^3$. Air is the working fluid; therefore, Sutherland's law is used to calculate the mean viscosity and $Pr=0.74$. Since $\langle H\rangle$ is not constant across the boundary layer, the mean temperature is measured independent of the mean velocity.

The governing equations [(1-7), (11), and (12)] are solved using the boundary-layer code of Ref. 4 with appropriate modifications made to implement the variable Pr_t model. A nonuniform grid is specified. It is found that a grid with 101 points is sufficient to give a grid-independent solution for all cases investigated. The boundary layer is assumed to be turbulent right from the leading edge of the plate and the built-in turbulence model in Ref. 4 is used to carry out the calculation up to $R_\theta=2\times10^2$, where the turbulence model under investigation takes over. This way, all model calculations start with the same initial conditions. Furthermore, all calculations are carried out to the measured R_θ, where meaningful comparisons with measurements are made.

The mean velocity and temperature results for the compressible cases with an adiabatic wall boundary condition are shown in Figs. 4 and 5. Three different ways of plotting the velocity results are presented: the conventional semilog plot (Fig. 4a), the semilog plot in van Driest[3] coordinates (Fig. 4b) and the linear plot (Fig. 5a). On the other hand, only a linear plot of the mean temperature is given in Fig. 5b because a friction temperature cannot be suitably defined for an adiabatic wall boundary condition. The rationale for presenting the mean velocity in these three different forms can be explained as follows. First, the conventional semilog plot for compressible flows has a density effect included in the definitions of u^+ and y_w^+, therefore, the true velocity profile prediction cannot be directly compared with measurements. Second, errors in the predictions of the mean temperature and hence the mean density can occur in such a way that they tend to mask the discrepancy in the semilog plots of the mean velocity. In view of this, it is also necessary to compare the mean velocity in a linear plot so that its actual agreement with measurements can be thoroughly analyzed. Third, van Driest[3] suggests stretching u^+ further by a density ratio so that a new u_c^+ can be defined as:

$$u_c^+ = \int_0^{u^+} (\bar\rho/\bar\rho_w)^{1/2}\, du^+$$

With this new coordinate, the compressible law of the wall as deduced by van Driest[3] and simplified by Bradshaw[5] can be written as:

$$u_c^+ = (1/0.41)\ \ell n\, y_w^+ + 5.2 + 95M_t^2$$

This form differs from the conventional law of the wall which is given by $u^+ = (1/0.41)\ \ell n\, y_w^+ + B$, where the constant B is a function of Mach number for compressible boundary-layer flows. When the velocity results are plotted in both u^+ and u_c^+ forms, the validity and extent of these log laws can be analyzed. Finally, the model calculations of C_f values are also listed in the figures for comparison with data.

It can be seen that the variable Pr_t model calculations of C_f are in good agreement with measurements and the predictions of constant Pr_t models. Both approaches yield a higher C_f for the case with $M_\infty=4.544$, whereas the predicted C_f values at higher M_∞ are in better agreement with measurements. The calculated mean profiles are in excellent agreement with data. This observation is true for flows with $M_\infty<5$ (Figs. 4a and 4b). It is not quite true for the case of $M_\infty=10.31$, where the variable Pr_t model gives a discernible and significant improvement in the predictions of both mean velocity and temperature (Figs. 5a and 5b) over those of the constant Pr_t models. The discrepancies between the k-ϵ and k-ω models can be attributed to the fact that the k-ω model is not asymptotically

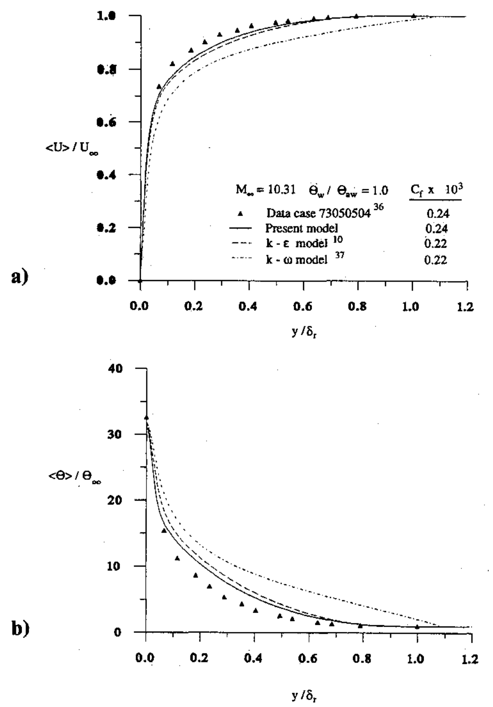

Fig. 5 Comparison of the calculated mean profiles with measurements for the $M_\infty=10.31$ adiabatic wall case: a) mean velocity in linear plot; and b) mean temperature in linear plot.

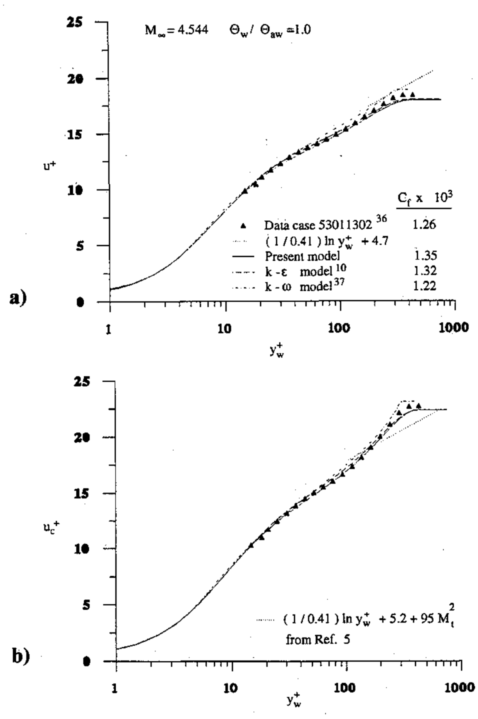

Fig. 4 Comparison of the calculated mean velocity with measurements for the $M_\infty=4.544$ adiabatic wall case: a) conventional law-of-the-wall plot; and b) van Driest compressible law-of-the-wall plot.

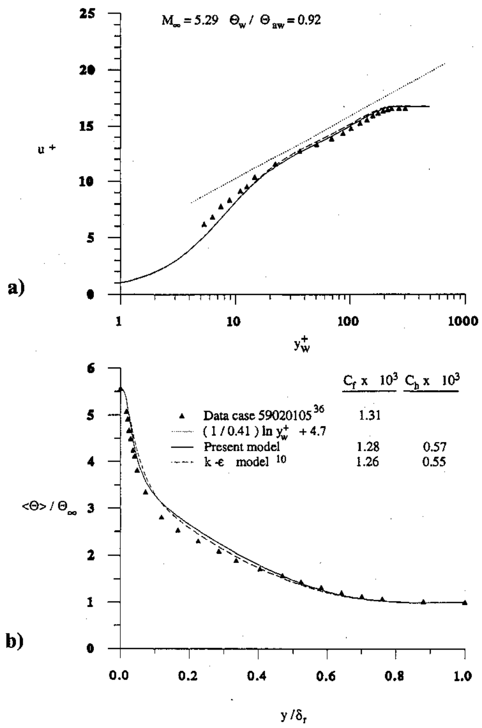

Fig. 6 Comparison of the calculated mean profiles with measurements for the $M_\infty = 5.29$ cooled wall case: a) conventional law-of-the-wall plot; and b) mean temperature in linear plot.

consistent near a wall. On the other hand, the improvement of the variable Pr_t model is due to a better estimate of the Pr_t near the wall.

Zhang et al.[10] have demonstrated that the calculated u^+ can be described fairly well by the conventional law of the wall and the constant B thus deduced is approximately 4.7 for the two cases examined. The present results are in agreement with their conclusion (Fig. 4a). Plots of the mean velocities in van Driest coordinates for the case with $M_\infty = 4.544$ are shown in Fig. 4b together with a plot of $u_c^+ = (1/0.41)\ \ell n\ y_w^+ + 5.2 + 95M_t^2$. A line parallel to this log law can be drawn through some of the data points; however, the intercept thus deduced is different. On the other hand, the calculated profiles from the three different models are in very good agreement with data over a much wider range of y_w^+, and the slope of the log-law thus determined yields a von Kármán constant $\kappa = 0.35$, which is significantly smaller than a value of 0.41 quoted by Bradshaw.[5] Finally, the calculated $k^+/\epsilon^+(y_w^+)^2$ for both M_∞ is 0.5 when the constant Pr_t model is used. The variable Pr_t model yields $k^+/\epsilon^+(y_w^+)^2 = 0.5$ and $\theta^{+2}/\epsilon_\theta^+(y_w^+)^2 = 0.74$ for the $M_\infty = 4.544$ case and $k^+/\epsilon^+(y_w^+)^2 = 0.5$ and $\theta^{+2}/\epsilon_\theta^+(y_w^+)^2 = 0.70$ for the $M_\infty = 10.31$ case. Therefore, the asymptotic values for $k^+/\epsilon^+(y_w^+)^2$ and $\theta^{+2}/\epsilon_\theta^+(y_w^+)^2$ are recovered for adiabatic wall compressible boundary-layer flows.

The results for the cooled wall cases are shown in Figs. 6 and 7. When $\Theta_w/\Theta_{aw} = 0.92$ and $M_\infty = 5.29$, there is a slight but not very significant difference between the calculations of the k-ϵ models (Figs. 6a and 6b). The reason for this good correlation could be due to the fact that the boundary-layer flow is not that much different from the case with an adiabatic wall. Consequently, there is a close dynamic similarity between the thermal field and the velocity field. On the other hand, when Θ_w/Θ_{aw} decreases to 0.3 and M_∞ increases to 8.18, the difference between these two model calculations becomes more discernible (Figs. 7a and 7b). At the same time, both model results yield substantial improvement over those given by the k-ω model. When the constant Pr_t and variable Pr_t predictions of the mean temperature are compared, it can be seen that the most significant improvement comes in the region $0 \le y/\delta_r < 0.3$ (Fig. 7b). This is in contrast to the adiabatic wall case with $M_\infty = 10.31$, where the improvement is slight and occurs across the whole boundary layer (Fig. 5b). A major reason for the noted discrepancy in the calculations of the mean tennperature is the lack of dynamic similarity between the thermal field and the velocity field when $\Theta_w/\Theta_{aw} = 0.30$. Such a similarity exists for an adiabatic wall and accounts for the good general agreement between the predictions of the constant Pr_t and variable Pr_t models. This lack of similarity further compounds the inaccuracy when the near-wall model is not asymptotically consistent as evidence by the predictions of the k-ω model (Fig. 7b).

This observation also applies to the predictions C_f and C_h. It is not possible to extract the measured C_h from the data in the case where $\Theta_w/\Theta_{aw} = 0.92$, thus, it is not presented for comparison. The calculated C_f and C_h for this case are improved by the same amount compared to the constant Pr_t model results (Fig. 6b). However, the calculated C_f is in better agreement with data. The comparison between the three model calculations of C_f and C_h for the case with $\Theta_w/\Theta_{aw} = 0.30$ is shown in Fig. 7a. The best predictions of C_f and C_h are provided by the variable Pr_t model, whereas the worst are given by the k-ω model. As expected, the variable Pr_t model calculations of C_f and C_h are in better agreement with measurements. For example, the error in the prediction of C_f decreases from over 7% to about 1%. In both test cases, the asymptotic values for $k^+/\epsilon^+(y_w^+)^2$ and $\theta^{+2}/\epsilon_\theta^+(y_w^+)^2$ are determined to be 0.5 and 0.74, respectively. In view of these results, it can be said that Morkovin's hypothesis and the constant Pr_t assumption are valid for boundary-layer flows with an adiabatic wall and with M_∞ as large as 10. However, Morkovin's hypothesis is still valid for highly cooled wall compressible boundary layers when it is used to formulate a variable Pr_t model.

Sample comparisons of the turbulence properties in the near-wall region are shown in Figs. 8 and 9. Only k^+, ϵ^+ (Figs. 8a and 8b) and $\overline{uv}^+$, $\overline{v\theta}$ (Figs. 9a and 9b) for the $M_\infty = 10.31$ case are presented. At low Mach numbers, the predictions of these properties by the different k-ϵ models are essentially identical. Discrepancies begin to develop as the Mach number increases and as the temperature ratio decreases. In general,

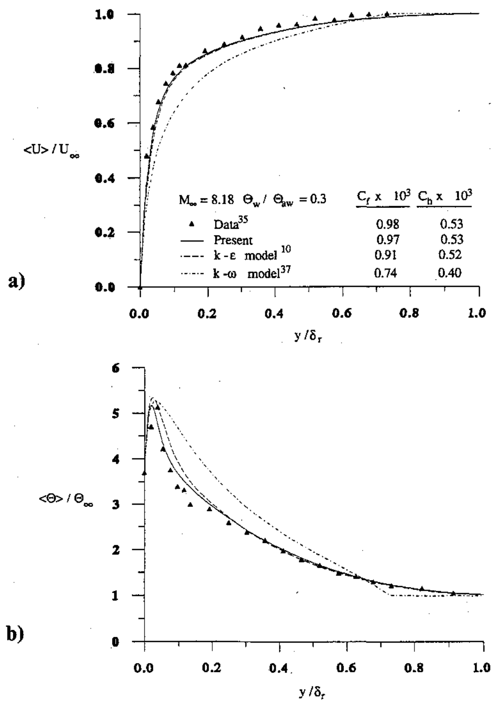

Fig. 7 Comparison of the calculated mean profiles with measurements for the $M_\infty = 8.18$ cooled wall case: a) mean velocity in linear plot; and b) mean temperature in linear plot.

the variable Pr_t model calculations of k^+ (Fig. 8a), ϵ^+ (Fig. 8b), $\overline{uv}^+$ (Fig. 9a), and $\overline{v\theta}$ (Fig. 9b) are slightly different than those predicted by the constant Pr_t model. The same behavior is observed for the cooled wall case at $M_\infty = 8.18$. One of the reasons is the variable turbulent Prandtl number. Plots of Pr_t across the boundary layers for the three test cases are shown in Fig. 10. The calculated Pr_t are seen to vary across the whole boundary layer and most rapidly in the near-wall region. It increases from a wall value of about 0.5 to a maximum of approximately 1.6 and then decreases to about 0.7 before it

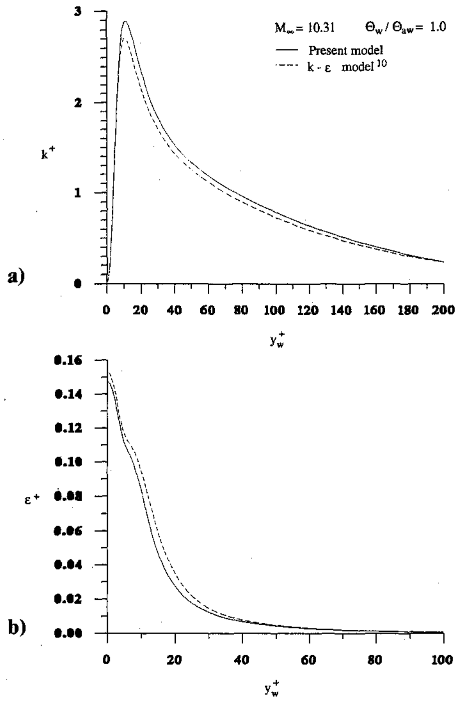

Fig. 8 Comparison of k^+ and ϵ^+ for the case with $M_\infty = 10.31$ and $\Theta_w/\Theta_{aw} = 1$: a) k^+; and b) ϵ^+.

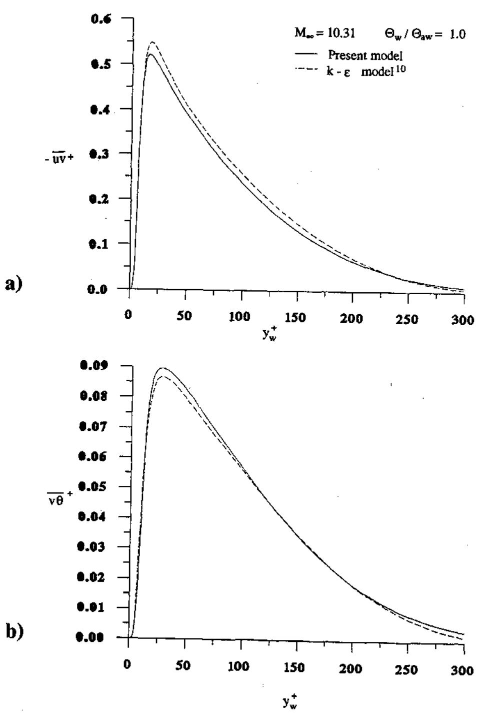

Fig. 9 Comparison of $\langle uv \rangle$ and $\langle v\theta \rangle$ for the case with $M_\infty = 10.31$ and $\Theta_w/\Theta_{aw} = 0.3$: a) $\langle uv \rangle$; and b) $\langle v\theta \rangle$.

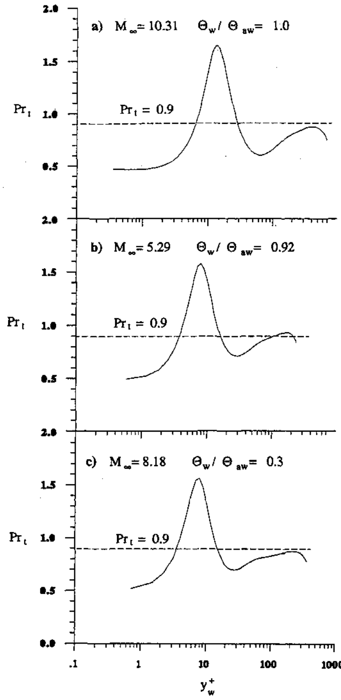

Fig. 10 Variation of Pr_t across the boundary layer for the three test cases.

increases to a value around 0.9 at $y_w^+ = 200$. Thereafter, Pr_t decreases slightly to about 0.8. This shows that large variations of Pr_t occur in the region $0 \leq y_w^+ = 200$. Consequently, it is not surprising to find that differences in the model calculations of k^+, ϵ^+, $\overline{uv}^+$, and $\overline{v\theta}$ also appear in the near-wall region.

Conclusions

A near-wall variable Pr_t turbulence model has been developed for the calculations of compressible flat plate turbulent boundary layers with constant heat flux and constant temperature wall boundary conditions. The model consists of solving four additional equations describing the transport of k, ϵ, θ^2, and ϵ_θ. The calculated values of k, ϵ, θ^2, and ϵ_θ are used to define the turbulent diffusivities of momentum and heat, and the assumption of a constant Pr_t is not required. These equations are modified for near-wall flow calculations so that they can be integrated directly to the wall and the exact boundary conditions at the wall are satisfied. The modifications of So et al.[15] for the k and ϵ equations are adopted and extended directly to compressible flows. Similar modifications for the incompressible form of the θ^2 and ϵ_θ equations[29] are carried out and they are extended to compressible flows by invoking Morkovin's hypothesis.[2] Thus formulated, the variable Pr_t model is internally consistent and asymptotically correct near a wall. The near-wall variable Pr_t model is used to calculate incompressible and compressible turbulent flows with free-stream Mach numbers as high as 10 and with adiabatic and cooled wall boundary conditions. Comparisons are made with DNS data, with experimental measurements, and with the predictions of other constant Pr_t models.

The analysis reveals that it is most important to have an asymptotically consistent near-wall model for the calculations of compressible boundary-layer flows. It also shows that Morkovin's hypothesis and the assumption of a constant Pr_t are essentially valid for adiabatic compressible boundary-layer flows with M_∞ as high as 10, but the constant Pr_t assumption is not as appropriate for compressible flows with highly cooled wall boundary condition. On the other hand, when the constant Pr_t assumption is relaxed while still invoking Morkovin's hypothesis in the formulation of an asymptotically consistent near-wall variable Pr_t model, the predictions of cooled wall compressible boundary-layer flows are improved. Consequently, it can be concluded that the assumption of dynamic similarity between compressible and incompressible flows is still valid, even for very high Mach number flows with adiabatic as well as cooled wall boundary conditions. However, the assumption of dynamic similarity between momentum and heat transport is not as applicable for highly cooled wall compressible boundary-layer flows. The calculated Pr_t is not constant and has a wall value of about 0.5 for all test cases considered. It increases sharply to approximately 1.6 away from the wall before it decreases to about 0.9 at $y_w^+ = 200$. Beyond $y_w^+ = 200$, Pr_t decreases slightly to about 0.8 at the edge of the boundary layer.

Acknowledgments

Funding support under Grant NAG-1-1080 from NASA Langley Research Center, Hampton, VA, is gratefully acknowledged. The grant is monitored by T. B. Gatski.

References

[1]Speziale, C. G., "Analytical Methods for the Development of Reynolds-Stress Closures in Turbulence," *Annual Review of Fluid Mechanics,* Vol. 23, 1991, pp. 107–157.

[2]Morkovin, M., "Effects of Compressibility on Turbulent Flows," *Mecanique de la Turbulence,* edited by A. Favre, Editors du Centre National de la Recherche Scientifique, Paris, 1962, pp. 367–380.

[3]van Driest, E. R., "Turbulent Boundary Layer in Compressible Fluids," *Journal of Aeronautical Sciences,* Vol. 18, No. 5, 1951, pp. 145–160, 216.

[4]Anderson, E. C., and Lewis, C. H., "Laminar or Turbulent Boundary-Layer Flows of Perfect Gases or Reacting Gas Mixtures in Chemical Equilibrium," NASA CR-1893, Oct. 1971.

[5]Bradshaw, P., "Compressible Turbulent Shear Layers," *Annual Review of Fluid Mechanics,* Vol. 9, 1977, pp. 33–54.

[6]Wilcox, D. C., "Reassessment of the Scale-Determining Equation for Advanced Turbulence Models," *AIAA Journal,* Vol. 26, No. 11, 1988, pp. 1299–1310.

[7]Speziale, C. G., and Sarkar, S., "Second-Order Closure Models for Supersonic Turbulent Flows," AIAA Paper 91-0217, 1991.

[8]Aupoix, B., and Cousteix, J., "Analysis of Turbulence Models for Hypersonic Boundary Layers," *Proceedings, 8th Turbulent Shear Flows,* Technical Univ. of Munich, Munich, Germany, Sept. 1991, pp. III-2.1–III-2.2.

[9]Bradshaw, P., Launder, B. E., and Lumley, J. L., "Collaborative Testing of Turbulence Models," *Journal of Fluids Engineering,* Vol. 113, March 1991, pp. 3–4.

[10]Zhang, H. S., So, R. M. C., Speziale, C. G., and Lai, Y. G., "Near-Wall Two-Equation Model for Compressible Turbulent Flows," *AIAA Journal,* Vol. 31, No. 1, pp. 196–199.

[11]Myong, H. K., and Kasagi, N., "A New Approach to the Improvement of the k-ϵ Turbulence Model for Wall Bounded Shear Flows," *JSME International Journal Series II,* Vol. 33, No. 1, 1990, pp. 63–72.

[12]Deng, G. B., and Piquet, J., "k-ϵ Turbulence Model for Low Reynolds Number Wall-Bounded Shear Flows," *Proceedings, 8th Turbulent Shear Flows,* Technical Univ. of Munich, Munich, Germany, Sept. 1991, pp. 26-2.1–26-2.6.

[13]Karlsson, R. I., Tinoco, H., and Svenson, U., "An Improved Form of the Near-Wall k-ϵ Model Based on New Experimental Data," *Proceedings, 8th Turbulent Shear Flows,* Technical Univ. of Munich, Munich, Germany, Sept. 1991, pp. 26-3.1–26-3.5.

[14]Michelassi, V., Rodi, W., and Scheuerer, G., "Testing a Low Reynolds Number k-ϵ Turbulence Model Based on Direct Stimulation Data," 8th Symposium on Turbulent Shear Flows, Paper 26-5, Munich, Sept. 9–11, 1991.

[15]So, R. M. C., Zhang, H. S., and Speziale, C. G., "Near-Wall Modeling of the Dissipation-Rate Equation," *AIAA Journal,* Vol. 29, No. 12, 1991, pp. 2069–2076.

[16]Yang, Z., and Shih, T. H., "A k-ϵ Modeling of Near Wall Turbulence," *Proceedings of the Fourth International Symposium on Computational Fluid Dynamics,* Univ. of California, Davis, CA, Sept. 1991, pp. 1305–1310.

[17]Kim, J., Moin, P., and Moser, R. D., "Turbulence Statistics in Fully Developed Channel Flow at Low Reynolds Number," *Journal of Fluid Mechanics,* Vol. 177, April 1987, pp. 133–186.

[18]Mansour, N. N., Kim, J., and Moin, P., "Reynolds-Stress and Dissipation-Rate Budgets in a Turbulent Channel Flow," *Journal of Fluid Mechanics,* Vol. 194, Sept. 1988, pp. 15–44.

[19]Spalart, P. R., "Direct Simulation of a Turbulent Boundary Layer up to $R_\theta = 1410$," *Journal of Fluid Mechanics,* Vol. 187, Feb. 1988, pp. 61–98.

[20]Lee, M. J., and Kim, J., "The Structure of Turbulence in a Simulated Plane Couette Flow," *Proceedings, 8th Turbulent Shear Flows,* Technical Univ. of Munich, Munich, Germany, Sept. 1991, pp. 5.3.1–5.3.6.

[21]Klebanoff, P. S., "Characteristics of Turbulence in a Boundary Layer with Zero Pressure Gradient," NACA TN-3178, July 1954.

[22]Nishino, K., and Kasagi, N., "Turbulence Statistics Measurements in a Two-Dimensional Channel Flow Using a Three-Dimensional Particle Tracking Velocimeter," *Proceedings, 7th Turbulent Shear Flows,* Stanford Univ., Stanford, CA, Sept. 1989, pp. 22.1.1–22.1.6.

[23]So, R. M. C., Lai, Y. G., Zhang, H. S., and Hwang, B. C., "Second-Order Near-Wall Turbulence Closures: A Review," *AIAA Journal,* Vol. 29, No. 11, 1991, pp. 1819–1835.

[24]Zhang, H. S., and So, R. M. C., "Asymptotically Correct Near-Wall Models for Boundary-Layer Flows," *Proceedings of the Fourth International Symposium on Computational Fluid Dynamics,* Univ. of California, Davis, CA, Sept. 1991, pp. 1348–1353.

[25]Zhang, H. S., So, R. M. C., and Zhu, M. L., "A Near-Wall Reynolds-Stress Turbulence Model and Its Application to Boundary-Layer Flows," (to be presented at the 31st AIAA Aerospace Sciences Meeting and Exhibit, Reno, NV, Jan. 11–14, 1993).

[26]Lai, Y.G., and So, R. M. C., "Near-Wall Modeling of Turbulent Heat Fluxes," *International Journal of Heat and Mass Transfer,* Vol. 33, No. 7, 1990, pp. 1429–1440.

[27]Nagano, Y., and Kim, C., "A Two-Equation Model for Heat Transport in Wall Turbulent Shear Flow," *Journal of Heat Transfer,* Vol. 110, No. 3, 1988, pp. 583–589.

[28]Nagano, Y., Tagawa, M., and Tsuji, T., "An Improved Two-Equation Heat Transfer Model for Wall Turbulent Shear Flows," *3rd ASME/JSME Thermal Engineering Conference Proceedings,* Vol. 3, June 1991, pp. 233–240.

[29]Sommer, T. P., So, R. M. C., and Lai, Y. G., "A Near-Wall Two-Equation Model for Turbulent Heat Fluxes," *International Journal of Heat and Mass Transfer,* (to be published).

[30]Shima, N., "A Reynolds-Stress Model for Near-Wall and Low-Reynolds-Number Regions," *Journal of Fluids Engineering,* Vol. 110, No. 1, 1988, pp. 38–44.

[31]Kim, J., and Moin, P., "Transport of Passive Scalars in a Turbulent Channel Flow," *Turbulent Shear Flows 6,* Springer-Verlag, Berlin, 1989, pp. 85–96.

[32]Kasagi, N., Tomita, Y., and Kuroda, A., "Direct Numerical Simulation of the Passive Scalar Field in a Two-Dimensional Turbulent Channel Flow," *3rd ASME/JSME Thermal Engineering Conference Proceedings,* Vol. 3, June 1991, pp. 175–182.

[33]Johnk, R. E., and Hanratty, T. J., "Temperature Profiles for Turbulent Flow of Air in a Pipe—I. The Fully Developed Heat Transfer Region," *Chemical Engineering Science,* Vol. 17, Nov. 1962, pp. 867–879.

[34]Hishida, M., Nagano, Y., and Tagawa, M., "Transport Processes of Heat and Momentum in the Wall Region of Turbulent Pipe Flow," *Proceedings of The Eighth International Heat Transfer Conference,* Vol. 3, Aug. 1986, pp. 925–930.

[35]Kussoy, M. I., and Horstman, K. C., "Documentation of Two- and Three-Dimensional Shock-Wave/Turbulent Boundary-Layer Interaction Flows at Mach 8.18," NASA TM-103838, 1991.

[36]Fernholz, H. H., and Finley, P. J., "A Critical Compilation of Compressible Turbulent Boundary Layer Data," AGARD No. 223, 1977.

[37]Wilcox, D. C., "Reassessment of the Scale-Determining Equation for Advanced Turbulence Models," *AIAA Journal,* Vol. 26, No. 11, 1988, pp. 1299–1310.

[38]Bradshaw, P., "The Effect of Mean Compression or Dilatation on the Turbulence Structure of Supersonic Boundary Layers," *Journal of Fluid Mechanics,* Vol. 63, April 1974, pp. 449–458.

[39]Antonia, R. A., and Kim J., "Turbulent Prandtl Number in the Near-Wall Region of a Turbulent Channel Flow," *International Journal of Heat and Mass Transfer,* Vol. 34, No. 7, 1991, pp. 1905–1908.